Pre-kinking analysis of a mixed-mode crack in a magnetoelectroelastic layer

Keqiang Hu[1,*], **Zengtao Chen**[1]

[1] Department of Mechanical Engineering, University of New Brunswick, Fredericton NB E3B 5A3, Canada
* Corresponding author: ckhu@unb.ca, keqianghu@163.com

Abstract A mixed-mode crack in a magnetoelectroelastic layer under in-plane mechanical, electric and magnetic loadings is considered for electrically and magnetically impermeable crack surface conditions. Fourier transforms are applied to reduce the mixed-boundary-value problem of the crack to a system of singular integral equations. The asymptotic fields near the crack tip are obtained in an explicit form and the corresponding field intensity factors are obtained. The exact solution for a crack in an infinite magnetoelectroelastic material can be recovered if the width of the layer tends to infinity. The crack kinking phenomenon is investigated by applying the criterion of maximum hoop stress intensity factors. The results show that the size of the layer and the electric and magnetic loadings have significant effects on the singular field distributions around the crack tip, and the hoop stress intensity factors are influenced by the material parameters, the electric loadings and the geometric size ratios.

Keywords Mixed-mode crack, Magnetoelectroelastic layer, Singular integral equations, Crack kinking, Hoop stress intensity factor

1. Introduction

In the recent decade, effect, magentoelectroelastic materials can be used in intelligent structures as sensors, actuators and transducers Owing to the unique magneto-electro-mechanical coupling effect. In the recent decade, there is a growing interest among researchers in solving fracture mechanics problems in magnetoelectroelastic media.

Crack initiation behavior in magnetoelectroelastic composite under in-plane deformation was investigated by Song and Sih [1]. Gao et al. [2] developed an exact treatment on the crack problems in a magnetoelectroelastic solid subjected to far-field loadings. Qin [3] obtained 2D Green's functions of defective magnetoelectroelastic solids under thermal loading, which can be used to establish boundary formulation and to analyze relevant fracture problems. The moving crack problem in an infinite size magnetoelectroelastic body under anti-plane shear and in-plane electro-magnetic loadings has recently been solved by Hu and Li [4] whose results predicted that the moving crack may curve when the velocity of the crack is greater than a certain value. The dynamic response of a penny-shaped crack in a magnetoelectroelastic layer was studied by Feng et al. [5]. Boundary element method was developed by Rojas-Díaz et al. [6] to study crack problem in linear magnetoelectroelastic materials under static loading conditions. Wang and Mai [7] discussed the different electromagnetic boundary conditions on the crack-faces in magnetoelectroelastic materials, which possess coupled piezoelectric, piezomagnetic and magnetoelectric effects. Zhong and Li [8] gave a magnetoelectroelastic analysis for an opening crack in a piezoelectromagnetic solid. Zhou and Chen [9] analyzed a partially conducting mode I crack in piezoelectromagnetic materials. Zhao and Fan [10] proposed a strip electric-magnetic breakdown model in magnetoelectroelastic medium to study the nonlinear character of electric field and magnetic field on fracture of magnetoelectroelastic materials. The problem of a planar magnetoelectroelastic layered half-plane subjected to generalized line forces and edge dislocations is analyzed by Ma and Lee [11]. Li and Lee [12] established real fundamental solutions for in-plane magnetoelectroelastic governing equations and studied collinear unequal cracks in magnetoelectroelastic materials. An embedded mixed-mode crack in a functionally graded magnetoelectroelastic infinite medium has been studied by Rekik et al. [13]. Recently, the pre-curving analysis of a crack in a magnetoelctroelastic strip under in-plane dynamic loading has been conducted by Hu and Chen [14] and the same authors [15] also studied the anti-plane problem of a magnetoelectroelastic strip sandwiched between elastic layers. The mode III crack crossing the magnetoelectroelastic bimaterial interface under concentrated magnetoelectromechanical loads was investigated by Wan et al. [16].

To the best knowledge of the authors, the mixed-mode crack in a magnetoelectroelastic layer with finite width under in-plane magneto-electro-elastic loadings has not been reported in the literature. This problem is solved in this paper. Fourier transforms are applied to reduce the mixed-boundary-value problem to a system of singular integral equations which can be solved numerically. The asymptotic fields near the crack tip are obtained in an explicit form and the corresponding field intensity factors are determined. The crack kinking phenomena is investigated by applying the criterion of maximum hoop stress intensity factors. The coupling magneto-electro-elastic effects on the crack-tip fields are investigated and the finite size effects on the dynamic fracture properties are discussed.

2. Problem statement and method of solution

Consider a transversely isotropic, linear magnetoelectroelastic material and denote the rectangular coordinates of a point by (x, y, z). The constitutive equations can be written as

$$\begin{Bmatrix}\sigma_{xx}\\ \sigma_{zz}\\ \sigma_{xz}\end{Bmatrix}=\begin{bmatrix}C_{11} & C_{13} & 0\\ C_{13} & C_{33} & 0\\ 0 & 0 & C_{44}\end{bmatrix}\begin{Bmatrix}\partial u_x/\partial x\\ \partial u_z/\partial z\\ \partial u_x/\partial z+\partial u_z/\partial x\end{Bmatrix}+\begin{bmatrix}0 & e_{31}\\ 0 & e_{33}\\ e_{15} & 0\end{bmatrix}\begin{Bmatrix}\partial\phi/\partial x\\ \partial\phi/\partial z\end{Bmatrix}+\begin{bmatrix}0 & h_{13}\\ 0 & h_{33}\\ h_{15} & 0\end{bmatrix}\begin{Bmatrix}\partial\varphi/\partial x\\ \partial\varphi/\partial z\end{Bmatrix}$$

$$\begin{Bmatrix}D_x\\ D_z\end{Bmatrix}=\begin{bmatrix}0 & 0 & e_{15}\\ e_{31} & e_{33} & 0\end{bmatrix}\begin{Bmatrix}\partial u_x/\partial x\\ \partial u_z/\partial z\\ \partial u_x/\partial z+\partial u_z/\partial x\end{Bmatrix}-\begin{bmatrix}\lambda_{11} & 0\\ 0 & \lambda_{33}\end{bmatrix}\begin{Bmatrix}\partial\phi/\partial x\\ \partial\phi/\partial z\end{Bmatrix}-\begin{bmatrix}d_{11} & 0\\ 0 & d_{33}\end{bmatrix}\begin{Bmatrix}\partial\varphi/\partial x\\ \partial\varphi/\partial z\end{Bmatrix} \tag{1}$$

$$\begin{Bmatrix}B_x\\ B_z\end{Bmatrix}=\begin{bmatrix}0 & 0 & h_{15}\\ h_{31} & h_{33} & 0\end{bmatrix}\begin{Bmatrix}\partial u_x/\partial x\\ \partial u_z/\partial z\\ \partial u_x/\partial z+\partial u_z/\partial x\end{Bmatrix}-\begin{bmatrix}d_{11} & 0\\ 0 & d_{33}\end{bmatrix}\begin{Bmatrix}\partial\phi/\partial x\\ \partial\phi/\partial z\end{Bmatrix}-\begin{bmatrix}\mu_{11} & 0\\ 0 & \mu_{33}\end{bmatrix}\begin{Bmatrix}\partial\varphi/\partial x\\ \partial\varphi/\partial z\end{Bmatrix}$$

where u_x, u_z are components of the displacement vector, ϕ and φ are the electric and magnetic potentials, respectively; $C_{11}, C_{13}, C_{33}, C_{44}$ are elastic constants, e_{15}, e_{31} are piezoelectric constants, h_{15}, h_{31} are piezomagnetic constants, $\lambda_{11}, \lambda_{33}$ are dielectric permittivities, and d_{11}, d_{33} are electromagnetic constants; σ_{ij}, D_i and B_i ($i, j = x, z$) are components of stress, electric displacement and magnetic induction, respectively.

We study an electrically and magnetically impermeable crack of length $2c$ in a magnetoelectroelastic layer of width $h_1 + h_2$, with the poling direction perpendicular to the crack plane, as shown in Fig. 1. Uniform normal stress P_0 and in-plane electric field E_0 and magnetic field H_0 are applied on the cracked layer. Symmetry conditions can be applied and then it is necessary to consider only the region ($x \geq 0$, $-h_2 \leq z \leq h_1$).

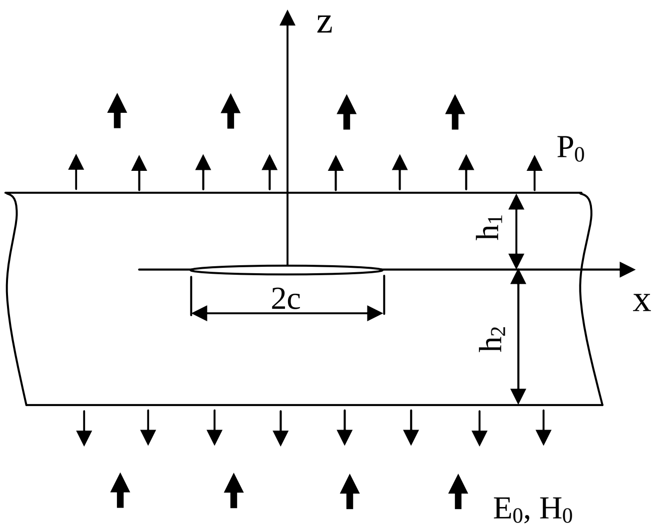

Figure 1. A cracked magnetoelectroelastic layer under in-plane magnetoelectromechanical loadings

Under the assumption of plane strain, the governing equations take the form

$$\begin{aligned}
&C_{11}u_{x,xx} + C_{44}u_{x,zz} + (C_{13} + C_{44})u_{z,xz} + (e_{31} + e_{15})\phi_{,xz} + (h_{31} + h_{15})\varphi_{,xz} = 0 \\
&(C_{13} + C_{44})u_{x,xz} + C_{44}u_{z,xx} + C_{33}u_{z,zz} + e_{15}\phi_{,xx} + e_{33}\phi_{,zz} + h_{15}\varphi_{,xx} + h_{33}\varphi_{,zz} = 0 \\
&(e_{31} + e_{15})u_{x,xz} + e_{15}u_{z,xx} + e_{33}u_{z,zz} - \lambda_{11}\phi_{,xx} - \lambda_{33}\phi_{,zz} - d_{11}\varphi_{,xx} - d_{33}\varphi_{,zz} = 0 \\
&(h_{31} + h_{15})u_{x,xz} + h_{15}u_{z,xx} + h_{33}u_{z,zz} - d_{11}\phi_{,xx} - d_{33}\phi_{,zz} - \mu_{11}\varphi_{,xx} - \mu_{33}\varphi_{,zz} = 0
\end{aligned} \tag{2}$$

The boundary conditions on the layer surfaces and the impermeable crack faces are:

$$\sigma_{zz}(x, h_1) = \sigma_{zz}(x, -h_2) = P_0 \qquad (0 \leq x < \infty) \tag{3}$$

$$\sigma_{zx}(x, h_1) = \sigma_{zx}(x, -h_2) = 0 \qquad (0 \leq x < \infty) \tag{4}$$

$$E_z(x, h_1) = E_z(x, -h_2) = E_0 \qquad (0 \leq x < \infty) \tag{5}$$

$$H_z(x, h_1) = H_z(x, -h_2) = H_0 \qquad (0 \leq x < \infty) \tag{6}$$

$$\sigma_{zz}(x,0) = 0,\ \ \sigma_{zx}(x,0) = 0 \qquad (0 \le x < c) \tag{7}$$

$$D_z(x,0) = 0,\ \ B_z(x,0) = 0 \qquad (0 \le x < c) \tag{8}$$

The continuity conditions for the physical quantities across the crack plane are:

$$\sigma_{zx}(x,0^+) = \sigma_{zx}(x,0^-),\ \ \sigma_{zz}(x,0^+) = \sigma_{zz}(x,0^-), \qquad (x \ge c) \tag{9}$$

$$D_z(x,0^+) = D_z(x,0^-),\ \ B_z(x,0^+) = B_z(x,0^-)\,, \qquad (x \ge c) \tag{10}$$

$$u_x(x,0^+) = u_x(x,0^-),\ \ u_z(x,0^+) = u_z(x,0^-)\,, \qquad (x \ge c) \tag{11}$$

$$\phi(x,0^+) = \phi(x,0^-),\ \ \varphi(x,0^+) = \varphi(x,0^-)\,, \qquad (x \ge c) \tag{12}$$

Fourier transforms are then applied on Eq. (2) and the solutions may be expressed as

$$u_{iz}^{(n)}(x,z) = \sum_{j=1}^{4} \Omega_{ij} \int_0^\infty \left[A_j^{(n)}(\xi)\cosh(\gamma_j \xi z) + B_j^{(n)}(\xi)\sinh(\gamma_j \xi z)\right]\cos(\xi x)d\xi + T_i z \qquad (i = 1-3) \tag{13}$$

$$u_x^{(n)}(x,z) = -\sum_{j=1}^{4} a_j \gamma_j \int_0^\infty \left[A_j^{(n)}(\xi)\sinh(\gamma_j \xi z) + B_j^{(n)}(\xi)\cosh(\gamma_j \xi z)\right]\sin(\xi x)d\xi \tag{14}$$

where $u_{1z} = u_z$, $u_{2z} = \phi$, $u_{3z} = \varphi$, $\Omega_{1j} = 1$, $\Omega_{2j} = b_j$, $\Omega_{3j} = d_j$, T_j $(j = 1,2,3)$ are constants and a_j, b_j, d_j $(j = 1-4)$ are known functions defined in Appendix A, $A_j^{(n)}(\xi)$, $B_j^{(n)}(\xi)$, $(n = 1,2;\ j = 1,2,3,4)$ are unknowns to be determined and the superscripts (1), (2) denote the fields quantities in the upper $0 \le y \le h_1$ and lower parts $-h_2 \le y \le 0$ of the cracked magnetoelectroelastic layer (as shown in Fig. 1), respectively.

The roots γ_j $(j = 1-4)$ are determined from solving the following characteristic equation:

$$\begin{vmatrix} C_{11} - C_{44}\gamma^2 & (C_{13} + C_{44})\gamma & (e_{31} + e_{15})\gamma & (h_{31} + h_{15})\gamma \\ (C_{13} + C_{44})\gamma & C_{33}\gamma^2 - C_{44} & e_{33}\gamma^2 - e_{15} & h_{33}\gamma^2 - h_{15} \\ (e_{31} + e_{15})\gamma & e_{33}\gamma^2 - e_{15} & \lambda_{11} - \lambda_{33}\gamma^2 & d_{11} - d_{33}\gamma^2 \\ (h_{31} + h_{15})\gamma & h_{33}\gamma^2 - h_{15} & d_{11} - d_{33}\gamma^2 & \mu_{11} - \mu_{33}\gamma^2 \end{vmatrix} = 0 \tag{15}$$

It is noted that the eighth-order characteristic equation (15) has eight roots which occur in pairs with the same magnitude but opposite signs, and for complex roots, the roots always appear in conjugate pairs. In the expressions (13, 14), the roots γ_j $(j = 1-4)$ are chosen as $\mathrm{Re}(\gamma_j) > 0$ by requiring a positive internal energy for the system to be in a steady state.

The expressions for the stresses, electric displacement and magnetic induction can be obtained as follows:

$$\sigma_{ix}^{(n)} = -\sum_{j=1}^{4} V_{ij} \int_0^\infty \xi\left[A_j^{(n)}(\xi)\cosh(\gamma_j \xi z) + B_j^{(n)}(\xi)\sinh(\gamma_j \xi z)\right]\sin(\xi x)d\xi \qquad (i = 1-3) \tag{16}$$

$$\sigma_{iz}^{(n)} = \sigma_{i0} - \sum_{j=1}^{4} U_{ij} \int_0^\infty \xi \left[A_j^{(n)}(\xi) \sinh(\gamma_j \xi z) + B_j^{(n)}(\xi) \cosh(\gamma_j \xi z) \right] \cos(\xi x) d\xi \quad (i = 1-4) \tag{17}$$

where

$$\begin{aligned}
&\sigma_{1x} = \sigma_{zx},\ \sigma_{2x} = D_x,\ \sigma_{3x} = B_x;\ V_{1j} = f_j,\ V_{2j} = s_j,\ V_{3j} = t_j \\
&\sigma_{1z} = \sigma_{zz},\ \sigma_{2z} = D_z,\ \sigma_{3z} = B_z,\ \sigma_{4z} = \sigma_{xx};\ U_{1j} = g_j,\ U_{2j} = m_j,\ U_{3j} = n_j,\ U_{4j} = q_j \\
&\sigma_{10} = P_0,\ \sigma_{20} = e_{33}T_1 - \lambda_{33}T_2 - d_{33}T_{33},\ \sigma_{30} = h_{33}T_1 - d_{33}T_2 - \mu_{33}T_3,\ \sigma_{40} = C_{13}T_1 + e_{31}T_2 + h_{31}T_3
\end{aligned} \tag{18}$$

and the coefficients are defined as:

$$\begin{aligned}
&f_j = C_{44}(a_j\gamma_j^2 + 1) - e_{15}b_j - h_{15}d_j,\ g_j = (C_{13}a_j + e_{33}b_j + h_{33}d_j - c_{33})\gamma_j \\
&q_j = (C_{11}a_j + e_{31}b_j + h_{31}d_j - c_{13})\gamma_j,\ m_j = (e_{31}a_j - \lambda_{33}b_j - d_{33}d_j - e_{33})\gamma_j \\
&n_j = (h_{31}a_j - d_{33}b_j - \mu_{33}d_j - h_{33})\gamma_j,\ s_j = e_{15}(a_j\gamma_j^2 + 1) + \lambda_{11}b_j + d_{11}d_j \\
&t_j = h_{15}(a_j\gamma_j^2 + 1) + d_{11}b_j + \mu_{11}d_j
\end{aligned} \tag{19}$$

From the boundary conditions (3-10), the unknown functions $B_j^{(1)}(\xi)$, $A_j^{(2)}(\xi)$, $B_j^{(2)}(\xi)$ $(j = 1-4)$ can be expressed by the four independent unknowns $A_j^{(1)}(\xi)$ $(j = 1-4)$ as

$$B_j^{(1)}(\xi) = \sum_{i=1}^{4} R_{ji}^{(1)}(\xi, h_1) A_i^{(1)}(\xi) \tag{20}$$

$$A_j^{(2)}(\xi) = \sum_{i=1}^{4} T_{ji}(\xi, h_1, h_2) A_i^{(1)}(\xi) \tag{21}$$

$$B_j^{(2)}(\xi) = \sum_{i=1}^{4} R_{ji}^{(2)}(\xi, h_2) A_i^{(2)}(\xi) = \sum_{i=1}^{4} Q_{ji}(\xi, h_1, h_2) A_i^{(1)}(\xi) \tag{22}$$

where $R_{ji}^{(1)}(\xi, h_1)$, $T_{ji}(\xi, h_1, h_2)$ and $R_{ji}^{(2)}(\xi, h_2)$ are known functions.

Introduce the auxiliary functions $\Phi_i(x)$ $(i = 1-4)$ such that

$$\begin{Bmatrix} \Phi_1(x) \\ \Phi_2(x) \\ \Phi_3(x) \\ \Phi_4(x) \end{Bmatrix} = \frac{\partial}{\partial x} \begin{Bmatrix} u_x^{(1)}(x,0^+) - u_x^{(2)}(x,0^-) \\ u_z^{(1)}(x,0^+) - u_z^{(2)}(x,0^-) \\ \phi^{(2)}(x,0^+) - \phi^{(1)}(x,0^-) \\ \varphi^{(2)}(x,0^+) - \varphi^{(1)}(x,0^-) \end{Bmatrix} \tag{23}$$

By applying the solutions (13, 14) and using the Fourier inverse transform, the unknowns can be obtained as

$$\begin{Bmatrix} A_1^{(1)}(\xi) \\ A_2^{(1)}(\xi) \\ A_3^{(1)}(\xi) \\ A_4^{(1)}(\xi) \end{Bmatrix} = -\frac{2}{\pi\xi} \begin{bmatrix} Y_{11}(\xi) & Y_{12}(\xi) & Y_{13}(\xi) & Y_{14}(\xi) \\ Y_{21}(\xi) & Y_{22}(\xi) & Y_{23}(\xi) & Y_{24}(\xi) \\ Y_{31}(\xi) & Y_{32}(\xi) & Y_{33}(\xi) & Y_{34}(\xi) \\ Y_{41}(\xi) & Y_{42}(\xi) & Y_{43}(\xi) & Y_{44}(\xi) \end{bmatrix} \begin{Bmatrix} \int_0^c \Phi_1(s)\cos(s\xi)ds \\ \int_0^c \Phi_2(s)\sin(s\xi)ds \\ \int_0^c \Phi_3(s)\sin(s\xi)ds \\ \int_0^c \Phi_4(s)\sin(s\xi)ds \end{Bmatrix} \tag{24}$$

where $Y_{ij}(\xi)$ $(i, j = 1-4)$ are known functions. Satisfaction of the mixed boundary conditions (7, 8) on the crack face plane leads to the simultaneous singular integral equations

$$\begin{aligned} &\int_{-1}^{1}\left\{\kappa_{i1}(s,x)\Psi_1(s)+\sum_{j=2}^{4}\left[\frac{U_{ij}^0}{s-x}+\kappa_{ij}(s,x)\right]\Psi_j(s)\right\}ds=-\pi\sigma_{i0}, \quad (i=1-3) \\ &\int_{-1}^{1}\left\{\left[\frac{U_{41}^0}{x-s}+\kappa_{41}(s,x)\right]\Psi_1(s,p)+\sum_{j=2}^{4}\kappa_{4j}(s,x)\Psi_j(s)\right\}ds=0 \end{aligned} \tag{25}$$

where $\Psi_i(s)=\Phi_i(cs)$, and $\kappa_{ij}(s,x)$ $(i=1-4)$ are known kernel functions, the constants U_{ij}^0 are defined as $U_{ij}^0=\lim\limits_{\xi\to\infty}U_{ij}(\xi)$, and $U_{ij}(\xi)$ are known functions. The functions $\Psi_i(s)$ $(i=1-4)$ satisfy the single-valuedness condition:

$$\int_{-1}^{1}\Psi_i(s)ds=0, \quad (i=1-4) \tag{26}$$

The solution of $\Psi_i(s)$ may be expressed as

$$\Psi_i(s)=H_i(s)\big/\sqrt{1-s^2} \tag{27}$$

where $H_i(s)$ $(i=1-4)$ are new unknowns to be solved.

The singular integral equations can be solved numerically as [17], [18]:

$$\begin{aligned} &\sum_{i=1}^{n}A_i\left\{[\kappa_{m1}(x_k,s_i)]H_1(s_i)+\sum_{j=2}^{4}\left[\frac{U_{mj}^0}{s_i-x_k}+\kappa_{mj}(x_k,s_i)\right]H_j(s_i)\right\}=-\pi\sigma_{m0}, \quad (m=1-3) \\ &\sum_{i=1}^{n}A_i\left\{\left[\frac{U_{41}^0}{x_k-s_i}+\kappa_{41}(x_k,s_i)\right]H_1(s_i)+\sum_{j=2}^{4}[\kappa_{4j}(x_k,s_i)]H_j(s_i)\right\}=0 \end{aligned} \tag{28}$$

where,

$$\begin{aligned} &s_i=\cos\left[\frac{(i-1)\pi}{n-1}\right], \quad (i=1,2,...,n); \quad x_k=\cos\left[\frac{(2k-1)\pi}{2(n-1)}\right], \quad (k=1,2,...,n-1) \\ &A_i=\frac{\pi}{2(n-1)}, \quad (i=1,n); \quad A_i=\frac{\pi}{(n-1)}, \quad (i=2,3,...,n-1) \end{aligned} \tag{29}$$

For $h_1,\ h_2\to\infty$, $\kappa_{ij}(s,x)=0$ and from (25) the exact solution can be obtained as

$$\Psi_1(s)=0,\ \ \Psi_i(s)=c_i s\big/\sqrt{1-s^2} \qquad (i=2-4) \tag{30}$$

where c_i $(i=2-4)$ are constants related to U_{ij}^0.

3. Asymptotic fields near the crack tip

Once the functions $H_j(s)$ $(j=1-4)$ are obtained from solving the algebraic equations (28), following the procedure in Li and Lee [19], the asymptotic solutions of the magnetoelectroelastic fields near the crack tip can be obtained by introducing a polar coordinate system (r,θ) with the origin at the right crack tip as

$$r=\sqrt{(x-c)^2+z^2}, \quad \theta=\tan^{-1}[z/(x-c)] \tag{31}$$

The hoop and shear stresses at an angle θ near the right tip of the crack are obtained from the following relations in terms of the polar coordinates (r,θ)

$$\begin{aligned}\sigma_{\theta\theta}(r,\theta)&=\sigma_{zz}(r,\theta)\cos^2\theta+\sigma_{xx}(r,\theta)\sin^2\theta-\sigma_{xz}(r,\theta)\sin 2\theta\\ \sigma_{r\theta}(r,\theta)&=\sin 2\theta[\sigma_{zz}(r,\theta)-\sigma_{xx}(r,\theta)]/2+\sigma_{xz}(r,\theta)\cos 2\theta\end{aligned} \tag{32}$$

Define the hoop stress intensity factor and shear stress intensity factor associated with the hoop and shear stresses at an arbitrary as angle θ as [20]:

$$K_{\theta\theta}=\lim_{r\to 0}\left(\sqrt{2r}\sigma_{\theta\theta}\right), \ K_{r\theta}=\lim_{r\to 0}\left(\sqrt{2r}\sigma_{r\theta}\right) \tag{33}$$

The hoop and shear stress intensity factors can be obtained as:

$$K_{\theta\theta}^{(n)}=\sqrt{c}\sum_{j=1}^{4}\left\{\begin{array}{l}H_1(1)Y_{j1}^0\left[(-1)^n\Lambda_{1j}(\theta)\left(g_j\cos^2\theta+q_j\sin^2\theta\right)-\Lambda_{2j}(\theta)f_j\sin 2\theta\right]\\ +\sum\limits_{k=2}^{4}H_k(1)Y_{jk}^0\left[(-1)^n\Lambda_{1j}(\theta)f_j\sin 2\theta+\Lambda_{2j}(\theta)\left(g_j\cos^2\theta+q_j\sin^2\theta\right)\right]\end{array}\right\} \tag{34}$$

$$K_{r\theta}^{(n)}=\sqrt{c}\sum_{j=1}^{4}\left\{\begin{array}{l}H_1(1)Y_{j1}^0\left[(-1)^n\Lambda_{1j}(\theta)\sin 2\theta\left(q_j-g_j\right)/2+\Lambda_{2j}(\theta)f_j\cos 2\theta\right]\\ +\sum\limits_{k=2}^{4}H_k(1)Y_{jk}^0\left[\Lambda_{2j}(\theta)\sin 2\theta\left(g_j-q_j\right)/2-(-1)^n\Lambda_{1j}(\theta)f_j\cos 2\theta\right]\end{array}\right\} \tag{35}$$

where $0\le\theta\le\pi$ when $n=1$ for the upper part and $-\pi\le\theta\le 0$ when $n=2$ for the lower part of the cracked layer, respectively; $Y_{ij}^0=\lim\limits_{\xi\to\infty}Y_{ij}(\xi)$, and the angular functions $\Lambda_{1j}(\theta)$ and $\Lambda_{2j}(\theta)$ $(j=1-4)$ are defined as

$$\Lambda_{nj}(\theta)=\sqrt{\frac{\sqrt{\cos^2(\theta)+\left[\gamma_j\sin(\theta)\right]^2}+(-1)^n\cos(\theta)}{2\left[\cos^2(\theta)+\left[\gamma_j\sin(\theta)\right]^2\right]}} \qquad (n=1,2) \tag{36}$$

By setting the angle θ equal to zero, the common expressions for the Mode-I and Mode-II stress intensity factors can be recovered

$$K_I=K_{\theta\theta}\big|_{\theta=0}=\sqrt{c}\sum_{j=1}^{4}g_j\sum_{k=2}^{4}Y_{jk}^0H_k(1), \ K_{II}=K_{r\theta}\big|_{\theta=0}=\sqrt{c}H_1(1)\sum_{j=1}^{4}f_jY_{j1}^0 \tag{37}$$

In this paper the criterion of maximum hoop stress intensity factors is applied to predict the crack kinking phenomena. It is noted that the applied electric and magnetic loadings and material properties have influence on the singular field near the crack tip, as shown in Eqs. (18), (25), (34), and (35).

4. Numerical results and discussions

For the magneto-electrically impermeable crack problem, the crack-tip fields are dependent on the remote mechanical, electrical and magnetic loading. To study the effect of magneto-electro-elastic interaction, the electric and magnetic loading parameters are introduced as:

$$L_E = e_{33}E_0/P_0\,, \quad L_H = h_{33}H_0/P_0 \tag{38}$$

The material constants used in the numerical calculation are selected as $BaTiO_3$-$CoFe_2O_4$ composite [21]:

$$\begin{aligned}
&C_{11} = 22.6\times10^{10}(\mathrm{N/m^2}),\ C_{13} = 12.4\times10^{10}(\mathrm{N/m^2}),\ C_{33} = 21.6\times10^{10}(\mathrm{N/m^2})\\
&C_{44} = 4.4\times10^{10}(\mathrm{N/m^2}),\ e_{15} = 5.8\ (\mathrm{C/m^2}),\ e_{31} = -2.2\ (\mathrm{C/m^2}),\\
&e_{33} = 9.3\ (\mathrm{C/m^2}),\ h_{15} = 275\ (\mathrm{N/Am}),\ h_{31} = 290.2\ (\mathrm{N/Am})\\
&h_{33} = 350\ (\mathrm{N/Am}),\ \lambda_{11} = 56.4\times10^{-10}(\mathrm{C^2/Nm^2}),\ \lambda_{33} = 63.5\times10^{-10}(\mathrm{C^2/Nm^2})\\
&\mu_{11} = 29.7\times10^{-5}(\mathrm{Ns^2/C^2}),\ \mu_{33} = 6.35\times10^{-5}(\mathrm{Ns^2/C^2})\\
&d_{11} = 5.367\times10^{-12}(\mathrm{Ns/VC}),\ d_{33} = 2737.5\times10^{-12}(\mathrm{Ns/VC})
\end{aligned} \tag{39}$$

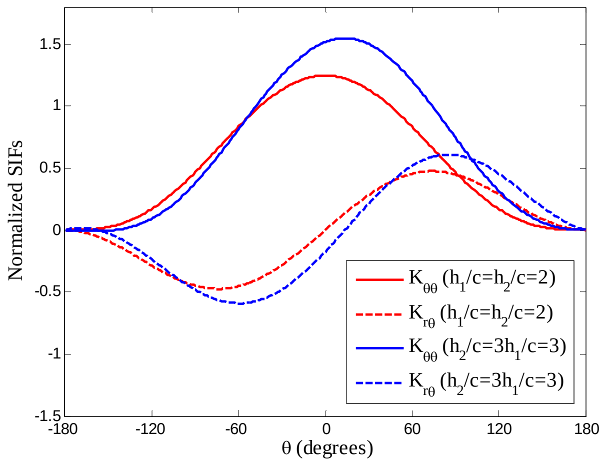

Figure 2. Normalized SIFs versus angle θ when $L_E = +0.5,\ L_H = -0.3$.

The variation of the normalized hoop and shear stress intensity factors (normalized by $P_0\sqrt{c}$) with angular position θ are displayed in Fig. 2. Without loss of generality, the applied stress is taken as $P_0 = 4.2\ \mathrm{MPa}$, and the magnitudes of the electric and magnetic loading parameters are chosen as $L_E = +0.5,\ L_H = -0.3$. The maximum hoop stress intensity factor (HSIF) occurs at $\theta = 0$ when the crack locates on the central plane of the layer, which indicates that the crack has a tendency to propagate along its original plane when the criterion of the maximum hoop stress intensity factor is applied. When $h_1 \neq h_2$, the maximum HSIF occurs at $\theta \neq 0$, which indicates that the crack has a tendency to deviate from its original plane. When the HSIFs reach the maximum, the magnitude of the SSIF is zero.

5. Concluding remarks

A mixed-mode crack in a magnetoelectroelastic layer under in-plane mechanical, electric and magnetic loadings is studied for impermeable crack surface conditions. Fourier transforms are applied to reduce the mixed-boundary-value problem of the crack to a system of singular integral equations. Asymptotic fields near the crack tip are obtained explicitly and the corresponding field intensity factors are defined. The analytic solution of the degenerated case for a cracked infinite magnetoelectroelastic solid is recovered when the width of the layer tends to infinity. The crack kinking phenomena is investigated by applying the criterion of maximum hoop stress intensity factors.

Appendix A

$$\mathrm{T}_1 = \left(P_0 + e_{33}E_0 + h_{33}H_0\right)/C_{33}, \ \mathrm{T}_2 = -E_0, \ \mathrm{T}_3 = -H_0 \tag{A.1}$$

$$\begin{Bmatrix} a_j \\ b_j \\ d_j \end{Bmatrix} = \begin{bmatrix} C_{11} - C_{44}\gamma_j^2 & e_{31} + e_{15} & h_{31} + h_{15} \\ (C_{13} + C_{44})\gamma_j^2 & e_{33}\gamma_j^2 - e_{15} & h_{33}\gamma_j^2 - h_{15} \\ (e_{31} + e_{15})\gamma_j^2 & \lambda_{11} - \lambda_{33}\gamma_j^2 & d_{11} - d_{33}\gamma_j^2 \end{bmatrix}^{-1} \begin{Bmatrix} C_{13} + C_{44} \\ C_{33}\gamma_j^2 - C_{44} \\ e_{33}\gamma_j^2 - e_{15} \end{Bmatrix} \tag{A.2}$$

References

[1] Z.F. Song, G.C. Sih, Crack initiation behavior in a magnetoelectroelastic composite under in-plane deformation. Theor Appl Fract Mech, 39 (2003) 189-207.
[2] C.F. Gao, K. Hannes, B. Herbert, Crack problems in magnetoelectroelastic solids. Part I: exact solution of a crack. Int J Eng Sci, 41 (2003) 969-981.
[3] Q.H. Qin, 2D Green’s functions of defective magnetoelectroelastic solids under thermal loading. Eng Anal Bound Elem, 29 (2005) 577-585.
[4] K.Q. Hu, G.Q. Li, Constant moving crack in a magnetoelectroelastic material under anti-plane shear loading. Int J Solids Struct, 42 (2005) 2823-2835.
[5] W.J. Feng, E. Pan, X. Wang, Dynamic fracture analysis of a penny-shaped crack in a magnetoelectroelastic layer. Int J Solids Struct, 44 (2007) 7955-7974.
[6] R. Rojas-Diaz, F. Garcia-Sanchez, A. Saez, C. Zhang, Fracture analysis of magnetoelectroelastic composite materials. Key Eng Mater, Advances in Fracture and Damage Mechanics VI, 348-349 (2007) 69-72.
[7] B.-L. Wang, Y.-W. Mai, Applicability of crack-face electromagnetic boundary conditions for fracture of magnetoelectroelastic materials. Int J Solids Struct, 44 (2007) 387-398.

[8] X.C. Zhong, X.F. Li, Magnetoelectroelastic analysis for an opening crack in a piezoelectromagnetic solid. Eur J Mech A/Solids, 26 (2007) 405-417.

[9] Z.G. Zhou, Z.T. Chen, Fracture mechanics analysis of a partially conducting mode I crack in piezoelectromagnetic materials. Eur J Mech A/Solids, 27 (2008) 824-846.

[10] M.-H. Zhao, C.-Y. Fan, Strip electric-magnetic breakdown model in magnetoelectroelastic medium. J Mech Phys Solids, 56 (2008) 3441-3458.

[11] C.-C. Ma, J.-M. Lee, Theoretical analysis of generalized loadings and image forces in a planar magnetoelectroelastic layered half-plane. J Mech Phys Solids, 57 (2009) 598-620.

[12] Y.D. Li, K.Y. Lee, Collinear unequal crack series in magnetoelectroelastic materials: Mode I case solved via new real fundamental solutions. Eng Fract Mech, 77 (2010) 2772-2790.

[13] M. Rekik, S. El-Borgi, Z. Ounaies, An embedded mixed-mode crack in a functionally graded magnetoelectroelastic infinite medium. Int J Solids Struct, 49 (2012) 835-845.

[14] K.Q. Hu, Z.T. Chen, Pre-curving analysis of an opening crack in a magnetoelectroelastic strip under in-plane impact loadings. J Appl Phys, 112, (2012) 124911.

[15] K.Q. Hu, Z.T. Chen, Dynamic response of a cracked magnetoelectroelastic layer sandwiched between two elastic layers. ZAMM Z Angew Math Mech, (2012) 1-12 DOI10.1002/zamm. 201200105.

[16]Y.P. Wan, Y.P. Yue, Z. Zhong, The mode III crack crossing the magnetoelectroelastic biomaterial interface under concentrated magnetoelectromechanical loads. Int J Solids Struct, 49 (2012) 3008-3021.

[17] P.S. Theocaris, N.I. Ioakimidis, Numerical integration methods for the solution of singular integral equations. Quart Appl Math, 35 (1977) 173-183.

[18] F. Delale, F. Erdogan, Effect of transverse shear and material orthotropy in a cracked spherical cap. Int J Solids Struct, 15 (1979) 907-926.

[19] X.F. Li, K.Y. Lee, Three-dimensional electroelastic analysis of a piezoelectric material with a penny-shaped dielectric crack. J Appl Mech, 71 (2004) 866-878.

[20] A. Azhdari, S. Nemat-Nasser, Hoop stress intensity factor and crack-kinking in anisotropic brittle solids. Int J Solids Struct, 33 (1996) 2023-2037.

[21] W.Y. Tian, R.K.N.D. Rajapakse, Fracture analysis of magnetoelectroelastic solids using path independent integrals. Int J Fract, 131 (2005) 311-335.